Published in final edited form as:
J Am Chem Soc. 2009 September 16; 131(36): 12994–13001. doi:10.1021/ja902712b.

Two-Photon Absorbing Nanocrystal Sensors for Ratiometric Detection of Oxygen

Emily J. McLaurin, **Andrew B. Greytak**, **Moungi G. Bawendi***, and **Daniel G. Nocera***
Department of Chemistry, 77 Massachusetts Avenue, Massachusetts Institute of Technology, Cambridge, Massachusetts 02139-4307, USA

Abstract

Two nanocrystal-osmium(II) polypyridyl (NC-Os(II)PP) conjugates have been designed to detect oxygen in biological environments. Polypyridines appended with a single free amine were linked with facility to a carboxylic acid functionality of a semiconductor NC overlayer to afford a biologically stable amide bond. The Os(II)PP complexes possess broad absorptions that extend into the red spectral region; this absorption feature makes them desirable acceptors of energy from NC donors. Fluorescence resonance energy transfer (FRET) from the NC to the Os(II)PP causes an enhanced Os(II)PP emission with a concomitant quenching of the NC emission. Owing to the large two-photon absorption cross-section of the NCs, FRET from NC to the Os(II)PP can be established under two-photon excitation conditions. In this way, two-photon processes of metal polypyridyl complexes can be exploited for sensing. The emission of the NC is insensitive to oxygen, even at 1 atm, whereas excited states of both osmium complexes are quenched in the presence of oxygen. The NC emission may thus be used as an internal reference to correct for fluctuations in the photoluminescence intensity signal. These properties taken together establish NC-Os(II)PP conjugates as competent ratiometric, two-photon oxygen sensors for application in biological microenvironments.

Introduction

Metabolic profiling of tumors provides a spatiotemporal map of the concentration profile of determinants of tumor growth, metabolism and response to therapy. Because the tumor microenvironment is generally characterized by hypoxia and acidity,[1] the concentration of protons and oxygen are especially important indicators of tumor health.[2] Understanding the dynamic relationship between pH and O_2 partial pressure (pO_2) in the tumor microenvironment during disease progression and treatment is critical to developing a heightened therapy response. For instance, combining antiangiogenic agents with other chemotherapies has yielded improved survival in cancer patients though the mechanism is not well understood.[3] Thus the non-invasive measurement of pH and pO_2 as a measure of tumor pathophysiology during drug delivery may offer a rational approach to the discovery of new and more efficacious cancer therapies. To do so, characterization of the tumor microenvironment requires the design of new sensors that dynamically respond to the modulation in the parameters under investigation. We have previously designed a self-referencing pH sensor to operate in biological microenvironments;[4] we now report here a self-referencing pO_2 sensor.

*mgb@mit.edu; nocera@mit.edu.

Supporting Information Available. Supporting information includes additional photophysical characterization of the Os(II)PP complexes and the NCs, additional two-photon studies, and GFC traces. This information is available free of charge via the Internet at http://pubs.acs.org/.

Fluorescent semiconductor NCs provide a basic scaffold for constructing biosensors. High quantum yields, photostability, narrow emission line-widths, and broad excitation profiles,[5-7] are some of the properties that have made NCs keystones of biosensing applications.[8,9] Attaching an analyte-sensitive fluorophore to the NC enables fluorescence resonance energy transfer (FRET) to be exploited as a signal transduction.[10-12] Sensing function of NCs in biology has expanded with the recent advent of (1) water-soluble, stable and bright NCs[13] and (2) the ability to modify the surface of NCs with coatings that do not affect the photophysical characteristics of the NC,[9] have minimal affect on the NC hydrodynamic radius,[14] and minimize the non-specific binding of the NCs to cellular structures.[15-17] This confluence of NC photophysical properties and surface derivatization methods has opened the way for the development of NC-conjugates for biosensing applications.[12,15,18-20]

The application of NC-conjugates for biosensing is bolstered by the proclivity of NCs to show high two photon absorption cross-sections.[21-23] Excitation and detection in dense biological samples, such as tissues, is best achieved using light in the near-IR (600 - 1000 nm), the so-called therapeutic window.[24] The spectral range may be accessed through this window by using a two-photon excitation source. For O_2 sensing in tissues, focused two-photon excitation allows for minimization of sampling volume with attenuated background contributions that arise from cellular auto-fluorescence and emission.[25,26] We have further emphasized the importance of establishing a ratiometric scheme for NC biosensing applications.[4] In this scheme, sensing action results from the engineered overlap of the dye absorption spectrum with an analyte-insensitive NC emission spectrum. Sensing can be quantified by referencing emission peak intensities (NC and dye conjugate) to the intensity of an isosbestic point, which functions as an internal reference. Self-referencing is preserved under a variety of optical conditions, making the method a robust sensing approach within a broad range of biological microenvironments.

Although there have been studies on both enhancement of two-photon induced phosphorescence through FRET and nanoparticle-based ratiometric oxygen sensors, so far they have been limited to studies using small molecule chromophores and nanoparticle-based polymer scaffolds.[27-32] We now report the design of an oxygen sensor incorporating a semiconductor nanocrystal (NC) that acts as both a scaffold, intensity standard and two-photon sensitizer for the Os(II)PP complexes (via FRET). Whereas polypyridyl complexes have been used pervasively as one-photon sensors, they have not been prominently exploited within a two-photon sensing construct owing to their relatively low two-photon absorption cross-sections.[33,34] We show here that the two-photon absorption cross-section can be enhanced by more than sixty-fold using NCs as a sensitizer according to the design illustrated in Scheme 1. This scheme permits metal polypyridyls to be implemented for routine two-photon sensing because the large two-photon excitation profile of the NC may be conferred upon Os(II)PP by utilizing FRET. Phosphorescence emission from the Os(II)PP complex is reversibly quenched in the presence of O_2 whereas the NC emission is unaffected because the FRET efficiency (NC→Os(II)PP) and the NC emission is unresponsive to O_2.[35] The NC emission thus affords an easily-resolved internal reference, allowing and Os(II)PP sensor to be used not only in the more typical lifetime detection mode,[36] but also in a ratiometric detection mode, thus offering the advantage of simple signal detection.

Experimental Section

Materials

The following chemicals were use as received: ammonium hexachloroosmate (NH_4OsCl_6), 4,7-diphenyl-1,10-phenanthroline (Ph_2phen), 2,2′-bipyridine (bpy), sodium hydrogen sulfite

($NaHSO_3$), 4,4′-dimethyl-2,2′-bipyridine, selenium dioxide (SeO_2), 4-dimethyl-aminopyridine (DMAP), *tert*-butyl 6-aminohexylcarbamate, triethylamine (TEA), ammonium hexafluorophosphate (NH_4PF_6), hexafluorophosphoric acid (HPF_6, 60% in water), polyacrylic acid (PAA), n-octylamine, N-hydroxysuccinimide (NHS), 3-sulfo-N-hydroxysuccinimide (S-NHS), anhydrous N,N-dimethylformamide (DMF, 99%), tetramethylammonium hydroxide, and rhodamine 6G from Sigma-Aldrich; selenium, silver nitrate ($AgNO_3$), diethylzinc, tri-n-octylphosphine (TOP, 97%), and dimethylcadmium from Strem; 1-ethyl-3-(3-dimethylamino-propyl)carbodiimide hydrochloride (EDC·HCl), hexamethyldisilathiane (Fluka); 1-hydroxy-benzotrizole (HOBt) (NovaBiochem); magnesium sulfate ($MgSO_4$) (EMD); trifluoroacetic acid (TFA, 99.9%) (J. T. Baker); and hexylphosphonic acid (HPA) (Alfa Aesar). Tri-n-octylphosphine oxide (TOPO) and hexadecylamine were distilled from 90% reagent grade materials (Sigma-Aldrich). 4′-methyl-2,2′-bipyridine-4-carboxylic acid (Cbpy),[37] *bis*(4,7-diphenyl-1,10-phenanthroline)osmium(II) dichloride [$Os(Ph_2phen)_2]Cl_2$ and *bis*(2,2′-bipyridine)-osmium(II) dichloride [$Os(bpy)_2]Cl_2$,[38] *tris*(2,2′-bipyridine)-ruthenium(II), *tris*(2,2′-bipyridine)-osmium(II), *bis*(2,2′-bipyridine)(4′-methyl-2,2′-bipyridine-4-carboxylic acid)-osmium (II) *bis*(hexafluoro-phosphate) [$Os(bpy)_2Cbpy](PF_6)_2$ and *bis*(4,7-diphenyl-1,10-phenanthroline)(4′-methyl-2,2′-bipyridine-4-carboxylic acid)osmium(II) *bis*(hexafluorophosphate) [$Os(Ph_2phen)_2Cbpy](PF_6)_2$ [39] were prepared as previously described.

Tert-butyl-6-(4′-methyl-2,2′-bipyridine-4-carboxamido)hexylcarbamate (Nbpy-BOC)—Cbpy (0.5051 g, 2.350 mmol, 1 eq), EDC·HCl (0.9049 g, 4.720 mmol, 2 eq), HOBt (0.6332 g, 4.686 mmol, 2 eq), DMAP (0.0583 g, 0.4772 mmol, <1 eq) and N-BOC-1,6-diaminohexane (1.1952 g, 5.5250 mmol, 2.3510 eq) were combined in methylene chloride (150 mL) containing 0.1 mL of TEA under N_2 overnight. The solution was then washed with water (4 × 100 mL), dried over $MgSO_4$, and the solvent was removed by rotary evaporation. The solid was dissolved in a few mL of ethyl acetate, loaded onto a Chromatotron plate (alumina, 2 mm), and eluted with ethyl acetate. The first band to elute was collected and the solvent removed *in vacuo* yielding 0.4986 g of the white ligand (51.43%). ^{1}H NMR (300 MHz, CD_3OD, 25 °C) δ = 1.42, (s, 9H, *t*Bu), 1.47, (m, 6H, -CH_2-), 1.67 (m, 2H, -CH_2-), 2.41 (s, 3H, bpy-CH_3), 3.04 (t, 2H, amide-CH_2-), 3.42 (t, 2H, amide-CH_2-), 7.32 (d, 1H, bpy-H), 7.76 (d, 1H, bpy-H), 8.22 (s, 1H, bpy-H), 8.54 (d, 1H, bpy-H), 8.66 (m, 1H, bpy-H), 8.80 (d, 1H, bpy-H).

Bis(2,2′-bipyridine)(N-(6-aminohexyl)-4′-methyl-2,2′-bipyridine-4-carboxamide)-osmium(II) _bis_(hexafluorophosphate) [$Os^{II}(bpy)_2(Nbpy)](PF_6)_2$ (1)—1 was prepared using synthetic methods similar to those employed for the preparation of $[Os^{II}(bpy)_2Cbpy](PF_6)_2$.[39] $Os^{II}(bpy)_2Cl_2$ (0.1430 g, 0.2493 mmol, 1.000 eq) and Cbpy (0.1199 g, 0.2496 mmol, 1.001 eq) were combined in degassed ethylene glycol and heated at 90 °C under N_2 for 24 h. The solution was cooled to room temperature and a saturated aqueous solution of ammonium hexafluorophosphate (20 mL) was added to cause a dark solid to precipitate. The solid was isolated by filtration, washed with water, ether, and dried under vacuum overnight. The crude product was purified by column chromatography (neutral alumina) with 1:1 toluene:acetonitrile eluant. The *tert*-butylcarbamate (BOC) protecting group was removed by stirring the complex in 1:1 methylene chloride:trifluoroacetic acid (CH_2Cl_2:TFA, 10 mL) for 1 h, followed by removal of the solvent *in vacuo*. The product was dissolved in acetone (20 mL), precipitated upon addition of ether (100 mL), isolated by filtration, and dried under vacuum yielding a black-green solid (0.1328 g, 65.29). ^{1}H NMR (300 MHz, CD_3CN, 25 °C) δ = 1.36 (m, 6H, -CH_2-), 1.61 (m, 4H, -CH_2-), 2.61 (s, 3H, bpy-CH_3), 3.36 (m, 2H, amide-CH_2-), 7.16 (d, 1H, bpy-H), 7.29 (m, 4H, bpy-H), 7.42 (d, 1H, bpy-H), 7.63 (m, 4H, bpy-H), 7.71 (m, 2H, bpy-H), 7.84

(m, 4H, bpy-H), 8.48 (s, 4H, bpy-H), 8.68 (s, 1H, bpy-H), 8.99 (t, 1H, amide-H), 9.21 (s, 1H, bpy-H). MALDI-TOF Calcd. (Found): $[M - 2PF_6]^{2+}$ 816.29 (816.15); $M - BOC - PF_6]^{+}$ 1061.31 (1061.28); $[M - BOC - 2PF_6]^{2+}$ 916.35 (916.35).

***Bis*(4,7-diphenyl-1,10-phenanthroline)(N-(6-aminohexyl)-4′-methyl-2,2′-bipyridine-4-carboxamide)osmium(II) *bis*(hexafluorophosphate) $[Os^{II}(Ph_2phen)_2(Nbpy)](PF_6)_2$ (2)—**$Os(Ph_2phen)_2Cl_2$ (0.1111 g, 0.1198 mmol, 1.000 eq) and Cbpy (0.1158 g, 0.2410 mmol, 2.011 eq) were combined in degassed ethylene glycol and heated at 90 °C under N_2 for 24 h. The solution was cooled to room temperature and a saturated aqueous solution of ammonium hexafluorophosphate (20 mL) was added to precipitate a dark solid. The solid was isolated by filtration, washed with water, ether, and dried under vacuum overnight. The crude product was purified by column chromatography (neutral alumina) with 1:1 toluene:acetonitrile eluant. The *tert*-butylcarbamate (BOC) protecting group was removed by stirring the complex in 1:1 methylene chloride (CH_2Cl_2:TFA, 10 mL) for 1 h, followed by removal of the solvent *in vacuo*. The product was dissolved in acetone (20 mL), precipitated upon addition of ether (100 mL), isolated by filtration, and dried under vacuum as above to yield a black-brown solid (0.0376 g, 26.9%). ^1H NMR (300 MHz, CD_3CN, 25 °C) δ = 1.36 (m, 6H, -CH_2-), 1.61 (m, 4H, -CH_2-), 2.65 (s, 3H, bpy-CH_3), 3.39 (m, 2H, amide-CH_2-), 7.14 (d, 1H, bpy-H), 7.49 (d, 2H, ligand-H), 7.62 (m, 20H, phenyl-H), 7.68 (m, 4H, ligand-H), 7.87 (d, 1H, ligand-H), 8.00 (m, 2H, ligand-H), 8.18 (m, 6H, ligand-H), 8.74 (s, 1H, bpy-H), 8.95 (t, 1H, amide-H), 9.26 (s, 1H, bpy-H). MALDI-TOF Calcd. (Found): $[M - 2PF_6]^{2+}$ 1168.42 (1168.24); $[M - BOC - PF_6]^{+}$ 1413.43 (1413.15); $[M - BOC - 2PF_6]^{2+}$ 1268.47 (1268.16).

N-octylamine modified polyacrylic acid (PAA-OA)

PAA (0.4949 g, 1800 MW, 1.0 eq) was functionalized with 40% *n*-octylamine groups by adopting a previously reported method.[7] Briefly, the acid, NHS (0.0553 g, 0.4804 mmol, 0.1723 eq), and EDC (0.5436 g, 2.836 mmol, 1.017 eq) were combined in DMF (3 mL) under N_2 for 1 h, followed by addition of *n*-octylamine (0.6 mL, 3.6 mmol, 1.3 eq) and left stirring overnight. After the DMF was removed *in vacuo*, water (5 mL) was used to precipitate the polymer and tetramethylammonium hydroxide (0.7491 g, 4.135 mmol, 1.483 eq) was added to re-dissolve the solid, overnight. After washing the solution with ethyl acetate (3 × 20 mL), the polymer was precipitated with concentrated hydrochloric acid (HCl, 0.34 mL, 4.1 mmol, 1.5 eq), washed with water (2 × 3 mL), and dried *in vacuo*. Water (5 mL) and a sodium hydroxide solution (1.5 mL, 3 M) were added to the solid. Filtration and drying *in vacuo* yielded a somewhat sticky white solid (0.1848 g, 22.97%).

Tri-octylphosphineoxide-capped nanocrystals (TOPO-NCs)

$(Cd_xZn_{1-x}Se)Cd_yZn_{1-y}S$ core-shell nanocrystals (**TOPO-NC**) were prepared as previously reported.[40] Briefly, ZnSe NCs were prepared by rapidly injecting diethylzinc (0.7 mmol) and tri-n-octylphosphine selenide (TOPSe, 1 mmol) dispersed in tri-n-octylphosphine (TOP, 5 mL) into a round bottom flask containing degassed hexadecylamine (7 g) at 310 °C. The solution was immediately cooled to 270 °C and NC growth was allowed to proceed for 2 h to furnish a solution of ZnSe NCs (λ_{1stAbs} = 350 nm). Aliquots of 1/3 of the above ZnSe NC lot were further modified by slowly adding a solution of dimethylcadmium (0.5 mmol) and TOPSe (1.2 mmol) in TOP (1.2 mL) to the ZnSe NCs in a solvent of TOPO (16 g) and hexylphosphonic acid (HPA, 4 mmol) under N_2 at 160 °C. After stirring for 48 h, $Cd_xZn_{1-x}Se$ core shell NCs ($\lambda_{1st\ abs}$ = 473 nm, λ_{PLmax} = 513 nm, FWHM = 40 nm) were obtained. The NCs were isolated by precipitation twice with methanol. A $Cd_yZn_{1-y}S$ shell was grown by redissolving the NCs in TOPO (10 g) and HPA (2.4 mmol) and introducing a solution of dimethylcadmium, diethylzinc, and hexamethyldisilthiane (2 eq vs. total moles

metal added) in TOP (8 mL) dropwise at 150 °C. The NCs were annealed overnight (80 °C) to furnish **TOPO-NCs** (λ_{PLmax} = 548 nm, FWHM = 36 nm).

Water-soluble nanocrystals (NCs)

The **TOPO-NCs** (10 mg) were isolated by repeated precipitation from hexanes with methanol and re-dissolved in a minimal amount of $CHCl_3$. **PAA-OA** (50 mg) was dissolved in $CHCl_3$ (5 mL), added dropwise to the NC solution, and left stirring overnight. After removing the $CHCl_3$ by vacuum, sodium bicarbonate buffer (pH ~8.5, 2 mL) was added to redissolve the NCs. The solution was then centrifuged (3900 rpm × 5 min), decanted, and dialyzed (with 50 kDa MW cutoff spin concentrators, Millipore) to furnish aqueous NCs (λ_{PLmax} = 549 nm, FWHM = 27 nm, φ = 40%).

NC-1 and NC-2 conjugates

Two methods were employed in the synthesis of the conjugates. In the first method, a solution of NC (1.60×10^{-4} M, 1 mL) was combined with 2-(N-morpholino)ethanesulfonic acid (MES) buffer (1 mL). The acid groups on NC were converted to esters of NHS through addition of an EDC/NHS solution (0.5 mM in each, 1 mL) (10 min). The precipitate was isolated by centrifugation and dried under vacuum. The NC precipitates were dissolved in sodium bicarbonate buffer (1.5 mL) and solutions of either **1** (4.365 mM, 0.200 mL, 0.873 mmol) or **2** (1.712 mM, 0.400 mL, 0.685 mmol) in DMF (0.1 mg of each) were added. The solutions were left stirring overnight, dialyzed into pH 7 buffer (phosphate), and centrifuged to settle out any undissolved material. The second method used differed from the first in that a solution of NC (1.60×10^{-4} M, 100 μL) was combined an EDC/S-NHS solution (0.5 mM in each, 100 μL, PBS buffer) forming some precipitate. Typically, addition of the Os(II)PP complexes in aqueous solutions of millimolar concentrations followed by TEA (50 μL) yielded optically clear solutions. The solutions were left stirring for 90 min and then dialyzed into pH 8.3 buffer ($NaHCO_3$) and further isolated by gel filtration chromatography.

Physical measurements

^{1}H NMR spectra were recorded on a Varian Mercury 300 MHz NMR at the MIT Department of Chemistry Instrumentation Facility (DCIF) and externally referenced to tetramethylsilane. MALDI-TOF mass spectrometry was performed on a Bruker Omniflex instrument in the DCIF using dithranol as the matrix. The instrument was calibrated with a quadratic polynomial using a mixture of bradykinin fragment 1-7 (757.3997), angiotensin II (1046.5423), and P14R synthetic peptide (1533.8582) (Sigma) with dithranol as the matrix.

Gel filtration chromatography (GFC) was performed on an Akta Prime system (GE) with a Superose 6 crosslinked dextran column. The hydrodynamic radii of NCs and conjugates were estimated by comparing the elution volumes to those of protein molecular weight standards (Bio-Rad). The eluent from the column was detected with the UV absorbance at 280 nm and the fluorescence spectrum was recorded. One mL fractions were collected from a volume of 5 - 25 mL. Fractions were combined based on the GFC traces and further characterized.

UV-vis absorption spectra were recorded on a Spectral Instruments (SI) CCD array UV-vis spectrophotometer, a Cary 5000, or an HP 8453 diode array spectrophotometer. Steady-state emission spectra were recorded on an automated Photon Technology International (PTI) QM 4 fluorometer equipped with a 150-W Xe arc lamp and a Hamamatsu R2658 photomultiplier tube. Time resolved emission measurements for the NCs were made with a chirped-pulse amplified Ti:sapphire laser system using the frequency doubled (400 nm) pump light provided by a Ti:sapphire laser system (100 fs pulsewidth). The detector was a Hamamatsu C4334 Streak Scope streak camera that is previously described.[41] Time resolved emission

measurements of the osmium complexes were made with pump light provided by the third harmonic (355 nm) of a Quanta-Ray Nd:YAG laser (Spectra-Physics) running at 10 Hz. The pump light was passed through a BBO crystal and split into a visible frequency and an infrared frequency. Lifetime measurements employed both the pump and visible beams to excite samples. The infrared light was used as the excitation source for two-photon measurements. The beam was focused onto the sample using a 100 mm focal length lens. A 900 nm short-pass filter was placed between the sample and a mounted 600 μm fiber-optic cable with a collimating lens. The other end of the cable was attached to an Ocean Optics QE65000 Spectrometer from which spectra were recorded. Power measurements were made by harvesting 20% of the incident laser beam.

Relative quantum yields of samples, φ_{sam}, were calculated using $[Ru^{II}(bpy)_3](PF_6)_2$, $[Os^{II}(bpy)_3](PF_6)_2$ or rhodamine 6G (R6G) in water as the reference according to:

$$\Phi_{\text{sam}}=\Phi_{\text{ref}}\left(\frac{A_{\text{ref}}}{A_{\text{sam}}}\right)\left(\frac{I_{\text{sam}}}{I_{\text{ref}}}\right)\left(\frac{\eta_{\text{sam}}}{\eta_{\text{ref}}}\right)^2 \quad (1)$$

A is the measured absorbance, η is the refractive index of the solvent, I is the integrated emission intensity, and φ_{ref} is the emission quantum yield of the reference. φ_{ref} was taken to be 0.053 for $Ru(bpy)_3^{2+}$ and 0.90 for R6G in water.[42,43] Using $Ru(bpy)_3^{2+}$ as the emission standard, φ was determined to be 0.031 for $Os(bpy)_3^{2+}$ in water and used as an additional reference. Samples for phosphorescence quantum yield and time resolved spectroscopic measurements were freeze-pump-thaw degassed for 3 cycles to 10^{-6} torr. Unless otherwise noted, all spectroscopy was performed in reagent grade deionized water.

Energy transfer analysis

The efficiency of energy transfer from the NC to the osmium complex was evaluated using Förster analysis:

$$E=\frac{mk_{D-A}}{mk_{D-A}+\tau_D^{-1}}=\frac{mR_0^6}{mR_0^6+r^6} \quad (2)$$

where $k_{D\text{-}A}$ is the rate of energy transfer, r is the distance between the donor and acceptor, R_0 is the critical transfer distance or the distance at which half of the donor molecules decay by energy transfer, and m is the number of acceptor molecules per donor. Experimentally, E can be obtained as:

$$E=1-\frac{\tau_{D-A}}{\tau_D} \quad (3)$$

where τ_D is the lifetime of the NC donor alone and $\tau_{D\text{-}A}$ is the lifetime of the bound donor (**NC-1** or **NC-2**).

While E may be experimentally determined from the excited state lifetime quenching, additional information is needed to quantify R_0, r, and m:

$$R_0^6=\frac{9000\,(\ln 10)\,\kappa^2\Phi_D}{128\pi^5 N n^4}\int_0^\infty F_D(\lambda)\,\varepsilon_A(\lambda)\,\lambda^4 d\lambda=1.02\times 10^{-25}\Phi_D J \quad (4)$$

where κ^2 is the relative orientation factor of the dipoles, taken to be $^2/_3$, φ_D is the quantum efficiency of the donor, N is Avogadro's number, and n is the index of refraction of the

medium, which is taken to be 1.4 in aqueous solution. The constants may be incorporated into one value, which is simply multiplied by φ_D. Similarly, the latter half of the equation may be represented as J, the overlap integral, where $F_D(\lambda)$ is the normalized intensity of the donor and $\varepsilon_A(\lambda)$ is the extinction coefficient of the acceptor at λ[44,45]. R_o may thus be calculated for the overlap of the experimentally determined spectra.

The average number of osmium complexes attached to the donor, m, can be determined from the optical cross-sections of the donor and acceptor as well as the absorption spectra of the conjugated **NC-1** and **NC-2** systems. The absorption spectra of the conjugates may be taken as a sum of the absorption of the donor and acceptor. The donor:acceptor ratio and the concentrations of the conjugates may be calculated using the individual donor and acceptor absorption spectra, their known ε values, and Beer's law.

Results

Scheme 2 presents the synthetic method employed to furnish mono-amine-functionalized Os(II)PP compounds. The single amine embodies a design element that precludes cross-coupling between the osmium complexes and NCs. This asymmetric ligand modification works best when the reactants are heated at low temperature for long periods of time. The more frequently employed conditions of higher refluxing temperatures over shorter periods of time[46] produces the *tris*-substituted complexes as well as undesirable products, especially for the case of **2**. Initial attempts to form the mono-amine-functionalized osmium compound followed by attachment of a protected diamine were largely unsuccessful. Instead, the mono-carboxylated bpy ligand was first coupled to an amine so that it was suitable for facile carbodiimide coupling to a subsequent carboxylic acid. Carboxy-bpy was coupled to *tert*-butyl 6-aminohexylcarbamate by carbodiimide coupling to generate **N-BOC-bpy**. The osmium-dichloride synthons were heated with the **N-BOC-bpy** ligand in ethylene glycol to afford the protected Os(II)PP complexes. Purification by alumina chromatography, deprotection of the BOC group with TFA, and precipitation of the complex yielded the water soluble, mono-aminated osmium complexes **1** and **2**, as established by ^{1}HNMR, UV-vis and emission spectroscopy and MALDI-TOF mass spectrometry.

Known synthetic methods of water-soluble NCs were employed to ensure a bright and stable scaffold. Briefly, water-soluble NCs were synthesized from $Cd_xZn_{1-x}Se$ cores overcoated with $Cd_yZn_{1-y}S$ shells and their surfaces were modified with *n*-octylamine functionalized polyacrylic acid (**PAA-OA**). Conjugates were synthesized by using the carbodiimide coupling method shown in Scheme 3. Single NCs were appended with either **1** or **2** through the mono-amine functionality. GFC was used to separate and validate the purity of these conjugates. Characterization of these products is shown in Figure 1 along with that of mixtures in the absence of the coupling agent. The large absorption at 14.5 min is characteristic of the NCs. The fractions containing single, unaggregated NCs were collected and used in further analysis. Further analysis of these samples using GFC indicated they were unimodal peaks (see SI).

Purified NC conjugates were analyzed with UV-vis absorption spectroscopy, steady-state, and time-resolved emission spectroscopies. The spectroscopic properties for the Os(II)PP complexes and the NC are summarized in Table 1. The absorption spectra of the Os(II)PP complexes are dominated by metal-ligand charge transfer (MLCT) transitions that are typical of metal polypyridyl complexes. The MLCT absorption band appears in the higher energy region accompanied by a shoulder to the lower energy side of the band. As has been observed previously, the MLCT absorption band of **2** is broader and more intense than that of its bpy relative, **1**.[47] Excitation into the MLCT absorption manifold produces broad, featureless emission bands centered in the near infrared corresponding to excited states

characterized by mono-exponential decays. The emission maximum of **2** lies to higher energy than that of **1**. This is paralleled by a more intense emission and longer lifetime (τ_{em}). The NC absorption spectrum exhibits an band at 525 nm and the emission spectrum exhibits a Gaussian band centered at 549 nm (FWHM = 36 nm, φ_{em} = 40%). NC fluorescence decay was typically biexponential, as observed previously.[48]

The absorption spectra of **NC-1** and **NC-2** in Figure 2 match the composite sum of the NC and the Os(II)PP spectra. Accordingly, values of *m* (Table 2) were determined from the absorption spectra of **NC-1** and **NC-2** using the assumption that they were the sum of the absorptions of the free NC and Os(II)PP components. MLCT excitation (λ_{exc} = 450 nm) of the Os(II)PP complexes within **NC-1** and **NC-2** conjugates yields an Os(II)-based emission that shifts to wavelengths shorter, by 35 and 49 nm, respectively, than that of the free complexes (Figure 3). Selective excitation of the NC (λ_{exc} = 355 nm) shows no additional changes in the Os(II)-based emissions. Comparison with the isolated Os(II)PP complexes excited at the same wavelengths exhibit an increase of the Os(II)PP emission within the conjugate whereas emission from the NC center is attenuated (Figure 3).

The trend in the excited state lifetimes of the individual Os(II)PP and NC components as compared to the conjugates (see Table 1) concurs with the results of steady-state spectroscopy. The NC and the Os(II)PP centers of the conjugates both show biexponential decays.[48] The increase in the steady-state emission of the Os(II)PP center within the conjugate is accompanied by a correspondent lifetime enhancement by a factor of nearly one order of magnitude. These results are in accordance with (Os(II)PP-polymer systems, which also show 3-4-fold excited state lifetime enhancements.[49] In turn, the lifetimes of the NC centers of the conjugates are diminished as compared to the NC alone.

To further quantify the efficiency of energy transfer, a lifetime analysis of the NC and conjugate was performed. A sample of **NC-2** possessing a larger **NC:2** ratio (*m*) was employed for this study. The results of the lifetime analysis are summarized in Table 2. The 67% energy transfer efficiency of **NC-1** accounts for the decrease in the steady-state emission of NC upon conjugation (as observed in Figure 3a); an energy transfer efficiency of 50% was calculated for the new **NC-2** sample. The distance parameters of energy transfer, R_o and r listed in Table 2, were determined from eqs (2) and (4) using the listed Os(II)PP to NC ratios.

The two-photon emission of the brighter **NC-2** and **2** are compared in Figure 4. For the purpose of this comparison the excitation wavelength must be chosen to excite **2** as well as the NC in the conjugate. A 920-nm two-photon excitation wavelength was chosen because it can excite both the NC and Os(II)PP centers within **NC-2** (at 460 nm) and scattered light at this wavelength is easily filtered from the emission of **2**. Emission from **2** was only observed when conjugated to NC, despite similar concentrations of **2** in **NC-2** and in a mixture of the complex with NC (13 μM and 15 μM, respectively). Concentrations of more than 100 μM of **2** were required to observe any two-photon emission. Quadratic power dependences were found for both the emission of the NC and of **2** in the conjugate. These data are detailed in the SI.

Oxygen efficiently quenches both the steady-state and time-resolved emission profiles of the Os(II)PP component of the **NC-1** and **NC-2** conjugates. Conversely, emission from the NC center of the conjugate is unaffected. The O_2 sensitivity of the complexes was initially quantified by integration of the area of the Os(II)PP emission under vacuum and under 1 atm of O_2. **NC-1** exhibits a decrease in emission of 21% while emission from **NC-2** is slightly more attenuated (23%). Phosphorescence lifetime decay curves of **1** and **2** were best fit to a single exponential when unconjugated to NC and to a biexponential when conjugated to NC.

The long lifetime component of the biexponential fits was used to determine the O_2 sensitivity of the conjugates. Consistent with steady-state emission quenching results, the lifetime of the Os(II)PP excited state in the **NC-1** conjugate decreases by 18% whereas the lifetime of the Os(II)PP excited state in the **NC-2** conjugate decreases by 23% upon exposure to 1 atm O_2. Further investigation of the steady-state emission intensity attenuation of **NC-2** under multiple O_2 pressures yielded Figure 5. It can be seen that the emission of the NC center remains unchanged, whereas that of **2** decreases with increasing O_2 pressure. An O_2 quenching rate constant of the conjugate is most reliably obtained from a fit of the lifetimes according to Stern-Volmer relation,

$$\frac{\tau_0}{\tau} = 1 + k_q \tau_0 pO_2 \quad (5)$$

where τ_o and τ are the lifetimes in the absence and presence, respectively, of O_2 at different pressures, k_q is the quenching constant, and pO_2 is the O_2 pressure. The Stern-Volmer fit of the lifetime data over an O_2 pressure range of 0-760 torr is linear and a quenching rate constant of $k_q = 1.8 \times 10^9$ s^{-1} M^{-1} (3000 s^{-1} $torr^{-1}$) is obtained from the plot shown in the inset of Figure 5.

Discussion

The extensive knowledge accrued of the photophysical properties of metal polypyridyl complexes[50,51] provided the motivation for choosing **1** and **2** as O_2-sensing elements for a NC platform. **1** and **2** were conjugated to NCs via a carbodiimide linkage. Figure 1 shows the GFC traces obtained for mixtures of NC and **1** (Figure 1a) and NC and **2** (Figure 1b) in the presence (blue) and absence (red) of coupling agents. The peak centered at 14.5 min is characteristic of single NCs. Fractions containing single NCs were collected. Steady state emission spectra of the collected fractions confirm binding of **1** to the NC only when coupling agents were used. Compound **2** was present along with NC in the absence of coupling agent, indicating that **2** can non-specifically bind to the NC. Thus, the collected fractions of **NC-2** may contain non-specifically bound **2**. However, the **NC-2** fractions consistently contained more **2** than the purified mixtures of the NC and **2**. Additionally, no appreciable loss of **2** occurred from the conjugates over a period of several days.

Compounds **1** and **2** possess absorption profiles that extend well into the red spectral region, thus leading to good spectral overlap (i.e., large J in eq 4) with the 550-nm emission band of the NCs. Moreover, the separation of the emission band of **1** and **2** from the emission profile of the NC engenders facile and accurate ratiometric sensing. Compound **2** is a superior sensor owing to the longer lifetime of the complex arising from the more rigid framework afforded by diphenylphenanthroline ligand.[47] Notwithstanding, the lifetime is short enough that abbreviated wait times between measurements permits faster data collection as compared to compounds currently used to sense O_2 in biological environments.[52]

As revealed by the data in Table 1, which compiles the steady-state and time-resolved spectroscopic results of the materials used in this study, the emission of the Os(II)PP complexes blue-shifts upon conjugation to the NC. This blue-shift can be understood in the context of the physical properties of Os(II)PP excited states. MLCT excitation of metal polypyridyl complexes is associated with a marked increase in the molecular dipole owing to the intramolecular charge separation. For this reason, the emission energy and intensity are strongly dependent upon the polarity of the surrounding environment.[53,54] High polarity environments tend to lower the energy of the thermally equilibrated excited state, thus resulting in a red-shift of the emission; conversely, lower polarity environments tend to result in a blue-shift in the emission. The shift of the emission band of the Os(II)PP centers

to higher energy in the **NC-1** and **NC-2** constructs is consistent with exclusion of water from the solvation sphere of the Os(II)PP center upon conjugation to the encapsulating polymer of the NC. Attendant with the shift of the emission band to higher energy, the lifetime of the excited state also increases as is predicted by energy gap law considerations.[47]

Emission from the Os(II)PP center is significantly increased when conjugated to the NC. The perturbation of the emission spectra of the native Os(II)PP centers conjugated to the NC can be seen in Figures 3b and 3d. Little emission is observed from unconjugated Os(II)PP; consequently, sufficiently high concentrations of **1** and **2** were required for the quantification of the intensity differences of emission from Os(II)PP alone versus when conjugated to the NC. Similarly, high concentrations of NC conjugates (Figure 3a and c) were required for sufficient detection and accurate quantification of the FRET process. Of the two conjugates, the emission enhancement of **NC-2** was easiest to detect, as expected, since the ratio of NC to Os(II)PP and the spectral overlap between the absorption of Os(II)PP and the NC emission (overlap integral, *J*) is larger in **NC-2** than in **NC-1**. In fact, the quantum yield was enhanced from 1.3% to 23%, which is relatively high for room temperature phosphorescence. The shorter distance between NC and **2**, despite the larger size of **2**, is likely due to the greater hydrophobicity of **2** relative to **1**, thus allowing **2** to envelop itself in the hydrophobic interior of the polymer. This would allow for more efficient FRET at longer distances (eq 2 and 4) as well as the exclusion of water from the solvation sphere, leading to brighter Os(II)PP emission.

The conjugate architecture confers the benefits of the two-photon absorption properties of the NC to the Os(II)PP center. Evidence for the enhanced two-photon absorption is provided in Figure 4. Here emission from **2** is observed in the conjugate, but not for unconjugated **2**, despite similar Os(II)PP concentrations for the two experiments. This observation is consistent with the preservation of FRET from the NC to Os(II)PP under two-photon excitation conditions. The two-photon emission of **2** when unbound only becomes visible when a concentration of 100 μM is attained, and even then, the emission was very weak. Comparison of this emission with the emission of the bound **2** shows an enhancement of more than 60 times when **2** is conjugated to the NC.

The conspicuous response of the Os(II)PP centers to O_2 is contrasted by an insensitivity of the NC emission. By examining the emission intensities from the NC and Os(II)PP centers and comparing their ratios with varying O_2 concentration, a ratiometric measurement of O_2 is obtained. Since the NC and Os(II)PP emission peaks are well separated, a third point may be taken at the baseline between the two emission bands, thus eliminating errors due to autofluorescence and other causes of baseline variation. Initially, the amount of O_2 quenching was ascertained at the extremes of 0 and 760 mm Hg of O_2. Stern-Volmer analysis of the oxygen quenching of emission intensity and lifetime from the Os(II)PP center of **NC-2** conjugate yields an appreciable quenching rate constant. The observed quenching rate constant of $k_q = 3000\ s^{-1}\ torr^{-1}$ translates to $1.8 \times 10^9\ s^{-1}\ M^{-1}$. This value is commensurate with metal polypyridyl complexes bound to polymers and cyclodextrins.[55] The conjugation of the metal complex to the QD thus does not significantly occlude oxygen from interacting with the metal polypyridyl excited state.

In summary, a NC construct for O_2 sensing has been established based on a FRET signal transduction mechanism. The value of the NC construct comes from the differential responses of the NC and FRET dye acceptor. The NC emission remains constant with changing O_2 levels, while that of the Os(II)PP dye acceptor is quenched with increasing O_2 pressure. These differential responses provide a basis for a ratiometric O_2 sensing response. Moreover, the signal transduction and ratiometric properties are maintained under two-photon excitation. Such a sensor is attractive for highly scattering environments in biology,

and is mandatory for imaging in tumors. Whereas Stern-Volmer analysis shows the oxygen sensitivity of the conjugate spans the range 0-760 torr, oxygen pressures relevant for biological measurements range from 0-160 torr,[2,56] where the sensor has an admittedly low dynamic range. Thus, modification of the sensor to achieve information on oxygen levels in biology requires probes with longer lived excited states.

Supplementary Material

Refer to Web version on PubMed Central for supplementary material.

Acknowledgments

We would like to thank the NSF-MRSEC program (DMR-0117795) and made use of its shared user facilities, the Harrison Spectroscopy Laboratory and the MIT-Harvard NIH Center for Cancer Nanotechnology Excellence (1U54-CA119349) (M.G.B.) as well as the Army Research Office (W911NF-06-1-0101) (D.G.N.) and the National Institutes of Health (R01CA126642-02) for support of this research. We also thank Steven Reece for support through scientific discussions and assistance with Nd:YAG experiments, Elizabeth Young for assistance with the streak camera NC lifetime measurements, and Gautham Nair for assistance with Ti: sapphire-based two-photon measurements.

References

1. Vaupel P, Kallinowski F, Okunieff P. Cancer Res. 1989; 49:6449–6465. [PubMed: 2684393]
2. Helmlinger G, Yuan F, Dellian M, Jain RK. Nat. Med. 1997; 3:177–182. [PubMed: 9018236]
3. Jain RK. Science. 2005; 307:58–62. [PubMed: 15637262]
4. Snee PT, Somers RC, Nair G, Zimmer JP, Bawendi MG, Nocera DG. J. Am. Chem. Soc. 2006; 128:13320–13321. [PubMed: 17031920]
5. Murray CB, Norris DJ, Bawendi MG. J. Am. Chem. Soc. 1993; 115:8706–8715.
6. Chan WC, Maxwell DJ, Gao X, Bailey RE, Han M, Nie S. Curr. Opin. Biotech. 2002; 13:40–46. [PubMed: 11849956]
7. Wu XY, Liu HJ, Liu JQ, Haley KN, Treadway JA, Larson JP, Ge NF, Peale F, Bruchez MP. Nat. Biotech. 2003; 21:41–46.
8. Alivisatos AP. Nat. Biotech. 2004; 22:47–52.
9. Wun AW, Snee PT, Chan YT, Bawendi MG, Nocera DG. J. Mater. Chem. 2005; 15:2697–2706.
10. Clapp AR, Medintz IL, Mauro JM, Fisher BR, Bawendi MG, Mattoussi H. J. Am. Chem. Soc. 2004; 126:301–310. [PubMed: 14709096]
11. Goldman ER, Medintz IL, Whitley JL, Hayhurst A, Clapp AR, Uyeda HT, Deschamps JR, Lassman ME, Mattoussi H. J. Am. Chem. Soc. 2005; 127:6744–6751. [PubMed: 15869297]
12. Somers RC, Bawendi MG, Nocera DG. Chem. Soc. Rev. 2007; 36:579–591. [PubMed: 17387407]
13. Michalet X, Pinaud FF, Bentolila LA, Tsay JM, Doose S, Li JJ, Sundaresan G, Wu AM, Gambhir SS, Weiss S. Science. 2005; 307:538–544. [PubMed: 15681376]
14. Zimmer JP, Kim S-W, Ohnishi S, Tanaka E, Frangioni JV, Bawendi MG. J. Am. Chem. Soc. 2006; 128:2526–2527. [PubMed: 16492023]
15. Liu W, Howarth M, Greytak AB, Nocera DG, Ting AY, Bawendi MB. J. Am. Chem. Soc. 2008; 130:1274–1284. [PubMed: 18177042]
16. Clapp AR, Pons T, Medintz IL, Delehanty JB, Melinger JS, Tiefenbrunn T, Dawson PE, Fisher BR, O'Rourke B, Mattoussi H. Adv. Mat. 2007; 19:1921–1926.
17. Bentzen EL, Tomlinson ID, Mason J, Gresch P, Warnement MR, Wright D, Sanders-Bush E, Blakely R, Rosenthal SL. Bioconjugate Chem. 2005; 16:1488–1494.
18. Medintz IL, Clapp AR, Brunel FM, Tiefenbrunn T, Uyeda H. Tetsuo, Chang EL, Deschamps JR, Dawson PE, Mattoussi H. Nat. Mater. 2006; 5:581–589. [PubMed: 16799548]
19. Zhang CY, Yeh HC, Kuroki MT, Wang TH. Nat. Mater. 2005; 4:826–831. [PubMed: 16379073]
20. Medintz IL, Uyeda HT, Goldman ER, Mattoussi H. Nat. Mater. 2005; 4:435–446. [PubMed: 15928695]

21. Blanton SA, Dehestani A, Lin PC, Guyot-Sionnest P. Chem. Phys. Lett. 1994; 229:317–322.
22. Larson DR, Zipfel WR, Williams RM, Clark SW, Bruchez MP, Wise FW, Webb WW. Science. 2003; 300:1434–1436. [PubMed: 12775841]
23. Pu SC, Yang MJ, Hsu CC, Lai CW, Hsieh CC, Lin SH, Cheng YM, Chou PT. Small. 2006; 2:1308–1313. [PubMed: 17192978]
24. Richards-Kortum R, Sevick-Muraca E. Annu. Rev. Phys. Chem. 1996; 47:555–606. [PubMed: 8930102]
25. Helmchen F, Denk W. Nat. Meth. 2005; 2:932–939.
26. Zipfel WR, Williams RM, Webb WW. Nat. Biotech. 2003; 21:1369–1377.
27. Finikova OS, Chen P, Ou Z, Kadish KM, Vinogradov SA. J. Photochem. Photobiol. A. 2008; 198:75–84.
28. Wu C, Bull B, Christensen K, McNeill J. Angew. Chem. Int. Ed. 2009; 121:2779–2783.
29. Xu H, Aylott JW, Kopelman R, Miller TJ, Philbert MA. Anal. Chem. 2001; 73:4124–4133. [PubMed: 11569801]
30. Koo YL, Cao Y, Kopelman R, Koo SM, Brasuel M, Philbert MA. Anal. Chem. 2004; 76:2498–2505. [PubMed: 15117189]
31. Briñas RP, Troxler T, Hochstrasser RM, Vinogradov SA. J. Am. Chem. Soc. 2005; 127:11851–11862. [PubMed: 16104764]
32. Finikova OS, Troxler T, Senes A, DeGrado WF, Hochstrasser RM, Vinogradov SA. J. Phys. Chem. A. 2007; 111:6977–6990. [PubMed: 17608457]
33. Coe BJ. Acc. Chem. Res. 2006; 39:383–393. [PubMed: 16784216]
34. Lemercier G, Bonne A, Four M, Lawson-Daku LM. Compt. Rend. Chimie. 2008; 11:709–715.
35. Walker GW, Sundar VC, Rudzinski CM, Bawendi MG, Nocera DG. Appl. Phys. Lett. 2003; 83:3555–3557.
28. Vanderkooi JM, Maniara G, Green TJ, Wilson DF. J. Biol. Chem. 1987; 262:5476–5482. [PubMed: 3571219]
37. McCafferty DG, Bishop BM, Wall CG, Hughes SG, Mecklenberg SL, Meyer TJ, Erickson BW. Tetrahedron. 1995; 51:1093–1106.
38. Kober EM, Caspar JV, Sullivan BP, Meyer TJ. Inorg. Chem. 1988; 27:4587–4598.
39. Dupray LM, Meyer TJ. Inorg. Chem. 1996; 35:6299–6307.
40. Ivanov SA, Nanda J, Piryatinski A, Achermann M, Balet LP, Bezel IV, Anikeeva PO, Tretiak S, Klimov VI. J. Phys. Chem. B. 2004; 108:10625–10630.
41. Damrauer NH, Hodgkiss JM, Rosenthal J, Nocera DG. J. Phys.Chem. B. 2004; 108:6315–6321. [PubMed: 18950117]
42. Henderson LJ Jr. Cherry WR. J. Photochem. 1985; 28:143–151.
43. Magde D, Wong R, Seybold PG. Photochem. Photobiol. 2002; 75:327–334. [PubMed: 12003120]
44. Förster T. Ann. Phys. 1948; 2:55–75.
45. Lakowicz, JR. Principles of Fluorescence Spectroscopy. 3rd ed. Springer; New York: 2006.
46. Buckingham DA, Dwyer FP, Goodwin HA, Sargeson AM. Aust. J. Chem. 1964; 17:325–336.
47. Kober EM, Caspar JV, Lumpkin RS, Meyer TJ. J. Phys. Chem. 1986; 90:3722–3734.
48. Fisher BR, Eisler H-J, Stott NE, Bawendi MG. J. Phys. Chem. B. 2004; 108:143–148.
49. Clarke Y, Xu W, Demas JN, DeGraff BA. Anal. Chem. 2000; 72:3468–3475. [PubMed: 10952529]
50. Kober EM, Sullivan BP, Dressick WJ, Caspar JV, Meyer TJ. J. Am. Chem. Soc. 1980; 102:7383–7385.
51. Kalyansundaram, K. Photochemistry of Polypyridine and Porphyrin Complexes. Academic Press; San Diego, CA: 1992.
52. Dunphy I, Vinogradov SA, Wilson DF. Anal. Biochem. 2002; 310:191–198. [PubMed: 12423638]
53. Caspar JV, Meyer TJ. J. Am. Chem. Soc. 1983; 105:5583–5590.
54. Hauenstein BL Jr. Dressick WJ, Buell SL, Demas JN, DeGraff BA. J. Am. Chem. Soc. 1983; 105:4251–4255.

55. Sacksteder L, Lee M, Demas JN, DeGraff BA. J. Am. Chem. Soc. 1993; 115:8230–8238.
56. Finikova OS, Lebedev AY, Aprelev A, Troxler T, Gao F, Garnacho C, Muro S, Hochstrasser RM, Vinogradov SA. Chem. Phys. Chem. 2008; 9:1673–1679. [PubMed: 18663708]

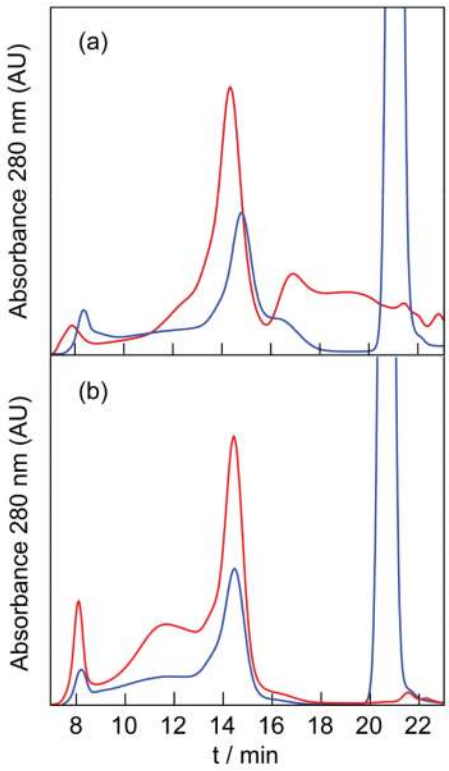

Figure 1.

A GFC trace of the conjugates **NC-1** and **NC-2** and the mixtures of the NC with **1** and NC with **2**. The GFC peaks recorded with a detection wavelength of 280 nm are shown in (a) **NC-1** ( ) and a mixture of the NC and **1** ( ) and (b) **NC-2** ( ) and a mixture of the NC and **2** ( ). The peak at 14.5 min is the elution peak for the single NCs.

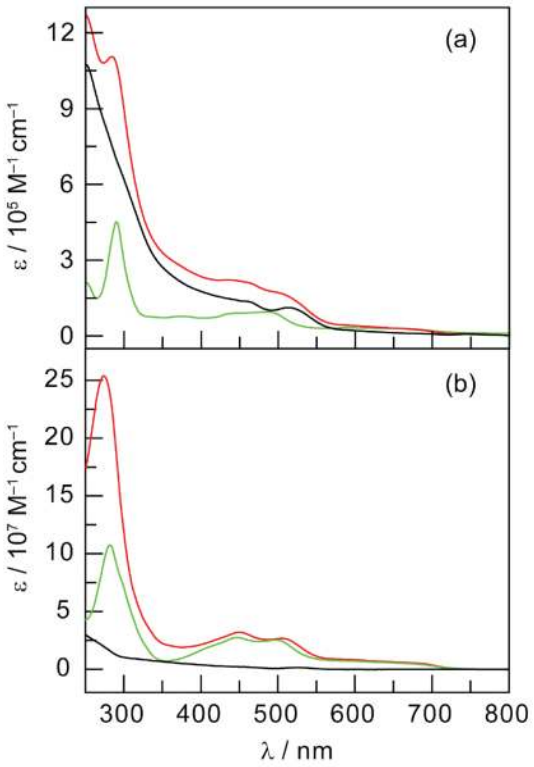

Figure 2.
(a) Absorbance of the NC (▬), **1** (▬) and the **NC-1** (▬) conjugate. (b) Absorbance of the NC (▬), **2** (▬) and the **NC-2** (▬) conjugate (1:135 NC:**2** ratio).

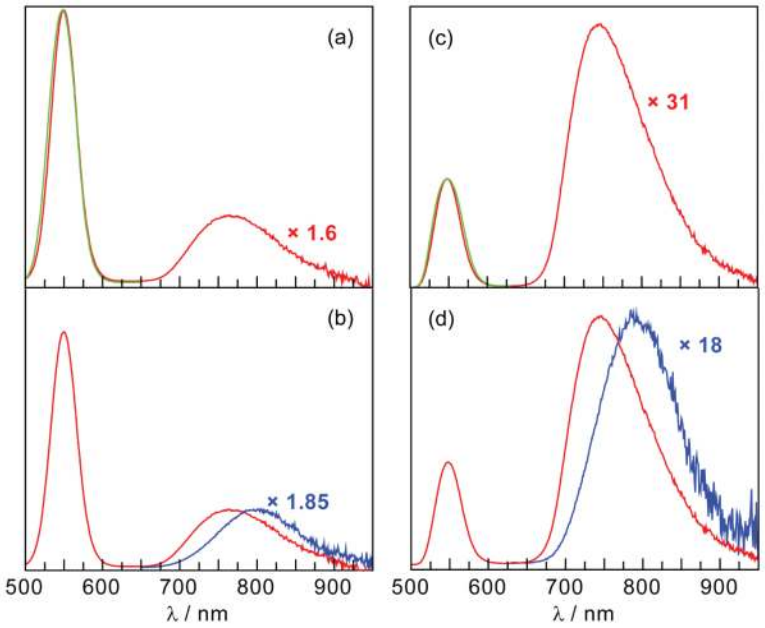

Figure 3.

Steady-state emission spectra (λ_{exc} = 450 nm) of the conjugates and their individual components in aqueous solution. Spectra were adjusted for concentration. (a) Spectra of the NC ( ) and the **NC-1** conjugate ( ) with the same NC peak intensity. (b) Spectra of **1** ( ) and **NC-1** ( ) with the same Os(II)PP emission peak intensity. (c) Spectra of the NC ( ) and **NC-2** ( ) (1:135 NC:**2** ratio) with the same NC peak intensity. (d) Spectra of **2** ( ) and **NC-2** ( ) with the same Os(II)PP emission peak intensity.

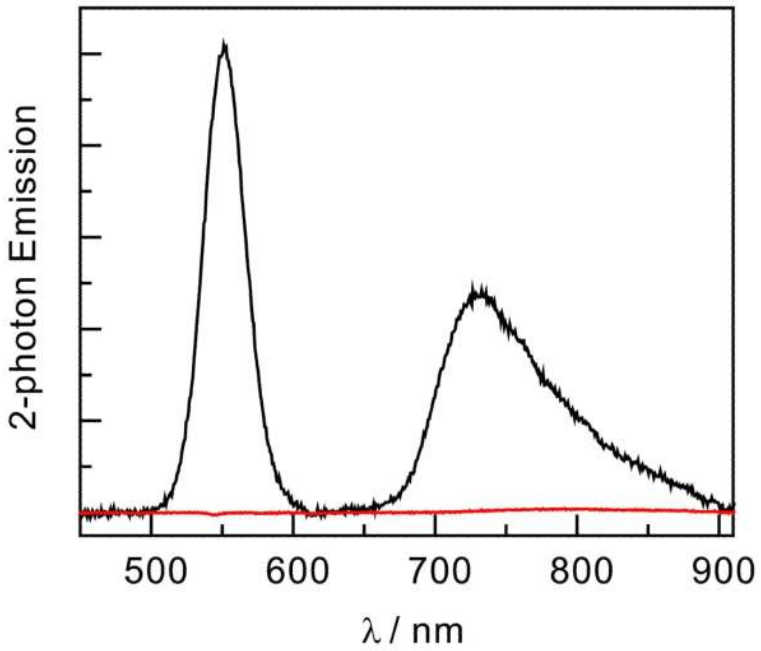

Figure 4.
Two-photon emission of **2** (▬) and the **NC-2** (▬) conjugate with the same Os(II)PP concentration.

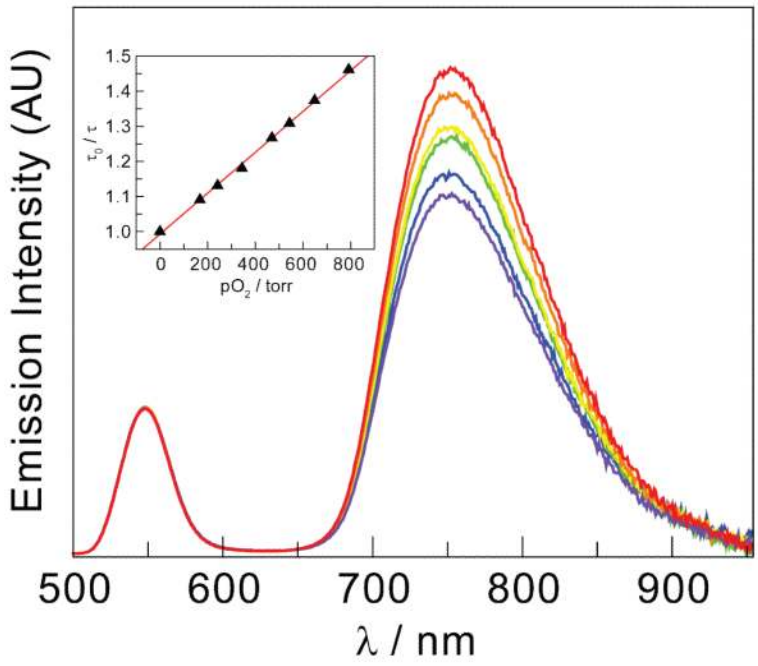

Figure 5.

Emission from the Os(II)PP center of the **NC-2** conjugate in the presence of 0 ( ), 133 ( ), 233 ( ), 382 ( ), 551 ( ), and 760 ( ) mmHg O_2. The inset shows the Stern-Volmer plot of the excited state lifetime of the Os(II)PP center in the **NC-2** conjugate vs. pO_2. The Stern-Volmer slope yields a quenching rate constant, $k_q = 1.8 \times 10^9$ s^{-1} M^{-1} (3000 s^{-1} $torr^{-1}$).

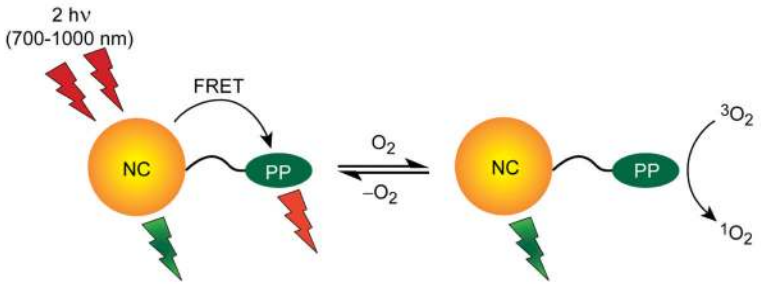

Scheme 1.

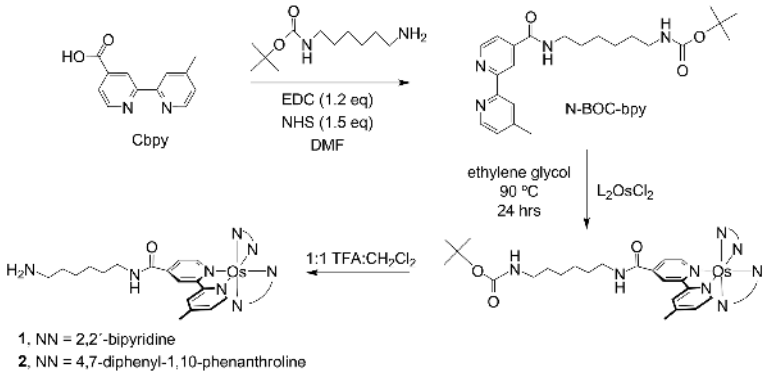

Scheme 2.

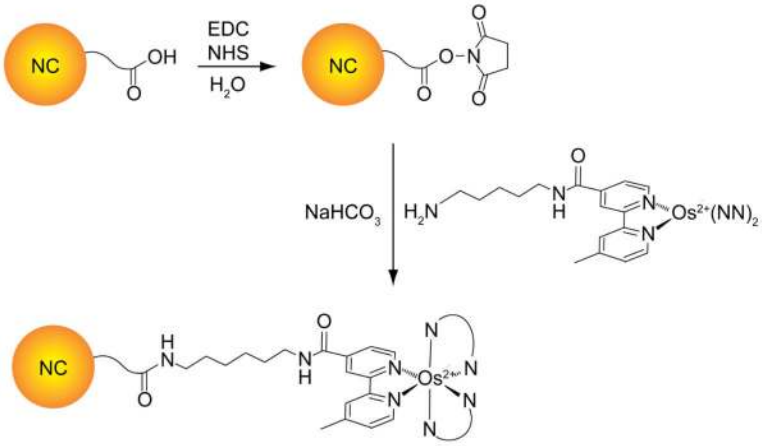

Scheme 3.

Table 1

Spectroscopic and Photophysical Properties of Os^{II} Polypyridyl Complexes, $(Cd_xZn_{1-x}Se)Cd_yZn_{1-y}S$ Core-Shell Nanocrystals, and Os^{II} Polypyridyl Complexes Conjugated with $(Cd_xZn_{1-x}Se)Cd_yZn_{1-y}S$ Core-Shell Nanocrystals in Aqueous Solution at Room Temperature.

Complex	λ_{abs} / nm	λ_{em} / nm	φ_{em}	τ_{em} / ns
$Os(bpy)_2(Nbpy)$ (**1**) [a]	490, ~650[c]	800	0.0096	12
$Os(DPPhen)_2(Nbpy)$ (**2**)[a]	450, ~625[c]	795	0.013	15
NC [b]	525[d]	549 [b]	0.40	18 [e]
NC- $Os(bpy)_2(Nbpy)$ (**NC-1**) [f]	435, 507, ~650[c]	549, 765	0.018,[g] 0.85[h]	6[e], 111[i]
NC-$Os(DPPhen)_2(Nbpy)$ (**NC-2**)[f]	445, 507, ~625[c]	549, 746	0.23,[g] 19.46[h]	9[e], 163[i]

[a] λ_{exc} = 450 nm, λ_{det} = 700 nm.

[b] λ_{exc} = 355 nm, λ_{det} = 550 nm.

[c] Shoulder.

[d] Lowest energy exciton peak

[e] λ_{exc} = 400 nm, λ_{det} = 550 nm.

[f] λ_{exc} = 355 nm, λ_{det} = 750 nm.

[g] Estimated from the enhancement factor (Figure 3).

[h] Increase in the Os(II)PP emission, normalized by Os(II)PP concentration, on going from the molecule alone to the conjugated molecule.

[i] λ_{exc} = 355 nm, λ_{det} = 750 nm and in the absence of O_2. Lifetimes were determined from the longer component of the bi-exponential emission fit.

Table 2

Förster energy transfer parameters for **NC-1** and **NC-2**

Complex	NC:Os(II)PP Ratio (m)[a]	r / nm[b]	R_0 / nm[c]	E[d]
NC-bpy_2OsNbpy (**NC-1**)	1:57	4.2	3.4	0.7
NC-$DPPhen_2$OsNbpy (**NC-2**)	1:13	4.0	4.0	0.5

[a] Approximate ratios determined from the absorption spectra of the conjugate assuming it to reflect the composite sum of the NC and Os(II)PP complex.

[b] Calculated from eq. (2).

[c] Calculated from eq. (4).

[d] Calculated from eq. (3).